Application Note

Biopharma

Agilent

Trusted Answers

# Advanced SEC with Online LS/DLS Detection for the Analysis of Lipid Nanoparticles CQAs

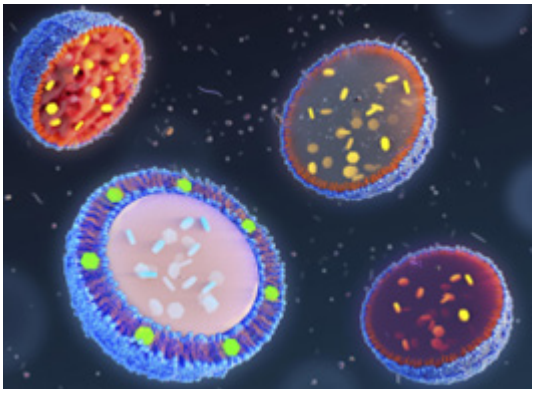


**Authors**

Johanna Simon and
Jenny Hong-Hoang
Merck Life Science KGaA,
Darmstadt, Germany

Sonja Schneider
Agilent Technologies,
Waldbronn, Germany



## Abstract

The size of lipid nanoparticles (LNPs) is a fundamental critical quality attribute (CQA) that directly impacts their biological performance. Precise control and analytical characterization of LNP size is essential for optimizing drug delivery systems and ensuring the safety and effectiveness of biopharmaceutical formulations.

In this application note, we present the size exclusion chromatography (SEC) analysis combined with online dynamic light scattering (DLS) and static light scattering (LS) of various LNP samples, including both loaded and empty vesicles. This approach yields precise and reproducible sizing data, along with information on stability and aggregation. A comparison with batch DLS measurements demonstrated a strong correlation with the online SEC-LS/DLS setup.

## Introduction

Innovative biopharmaceuticals like RNA-based modalities have gained immense attention over the last few years as advanced and powerful tools to combat different diseases. For a safe and highly efficient delivery of these fragile molecules, LNPs have emerged as promising delivery vehicles. To ensure safety and efficacy of the final drug product, the loaded LNPs need extensive analytical characterization. Besides lipid content and identity[1], aggregation and size are considered CQAs for LNPs, according to the United States Pharmacopeia (USP) guidelines.[2]

It has been reported that the hydrodynamic size of LNPs has severe effects on stability, biodistribution, circulation rate, and cellular uptake.[3,4] As stability of the LNPs is crucial to the effectiveness of the biopharmaceutical, instruments to measure the particle size are practical tools to control this property.

In this regard, SEC, in combination with advanced detection techniques like LS and DLS, can deliver deeper insightful information on chemistry and structure, complementing optical detection methods. Light scattering techniques provide information about molecular weight (MW), size, shape, as well as distribution of MW and size over the populations within a sample.

With the Agilent 1260 Infinity II Bio-SEC Multidetector System, the most comprehensive calculations are possible for molecular weight distribution, Mark-Houwink (M-H) plot for MW calculation, hydrodynamic radius (Rh) conformation, and radius of gyration (Rg). The 1260 Infinity II Bio-SEC Multidetector System combines static and dynamic light scattering detection, with a completely metal-free flow path. In combination with the biocompatible hardware of the 1290 Infinity III Bio LC for the SEC front end, the solution is optimally suited for the analysis of biomolecules. As the particles show scattering signals in UV detection[5], refractive index detection was added to enable quantification and calculation of radius of gyration using the refractive index increment (dn/dc). The Agilent 1260 Infinity III Refractive Index Detector provides excellent performance for UHPLC and HPLC experiments with rapid equilibration times and stable baselines.

Three SEC columns with varying pore sizes will be evaluated for peak shape, resolution, unspecific interaction, and particle bleeding into the DLS detector to find the optimal system setup. Different LNP samples (loaded and empty) will be analyzed to determine aggregation, size, shape, and the stability of the LNPs using the online SEC-LS/DLS setup.

## Experimental

### Equipment

Agilent 1290 Infinity III Bio LC System:

- Agilent 1290 Infinity III Bio Flexible Pump (G7131A)
- Agilent 1290 Infinity III Bio Multisampler (G7137A) with Sample Thermostat (option #101)
- Agilent 1290 Infinity III Multicolumn Thermostat (G7116B) with Quick Connect Bio Heat Exchanger Standard Flow (G7116-60071)
- Agilent 1260 Infinity III Refractive Index Detector (G7162A)
- Agilent 1260 Infinity II Bio-SEC Multidetector System featuring dual-angle and DLS detection (G7805AA and G7809A)

### Software

Agilent GPC/SEC Software version 2.2 or later versions

### Columns

- Agilent AdvanceBio SEC, 300 Å, 7.8 × 300 mm, 2.7 µm (part number PL1180-5301)
- Agilent Bio SEC-5, 2,000 Å, 7.8 × 300 mm, 5 µm (part number 5190-2541)
- Agilent PL aquagel-OH MIXED-H, 7.5 × 300 mm, 8 µm (part number PL1149-6800)

All three columns were extensively flushed with phosphate buffered saline (PBS) 24 hours before they were attached to the 1260 Infinity II Bio-SEC Multidetector System featuring dual-angle and DLS detection.

### Chemicals

Fresh ultrapure water was obtained from a Milli-Q Integral system equipped with a 0.22 µm membrane point-of-use cartridge (Millipak, Merck-Millipore, Billerica, MA, USA). The phosphate buffered saline (PBS) tablets and the bovine serum albumin (BSA) were purchased from Sigma-Aldrich, St. Louis, MO, USA. The prepared PBS buffer was filtered threefold using a 0.2 µm membrane filter.

BSA was dissolved in the filtered PBS buffer to a concentration of 20 mg/mL.

### Samples

Different LNPs samples, loaded and empty, plus a monoclonal antibody (mAb), were kindly provided by Merck Life Science KGaA, Darmstadt, Germany. LNP A and B differ in their lipid composition. All LNP samples were diluted in a ratio of 1:10 with the filtered PBS buffer and were immediately analyzed after dilution. In addition, the LNPs were exposed to several freeze-thaw cycles for stability testing. The mAb was injected without dilution.

### Method

**Table 1.** Chromatographic conditions.

| Parameter | Value |
|---|---|
| Isocratic | Triple-filtered PBS buffer in channel A<br>Flow rate: 0.6 mL/min<br>Stop time: 20 to 35 minutes |
| MCT Temperature | 30 °C |
| RI Detection | Temperature: 30 °C<br>Peak width: > 0.05 min (1s response time) (9.25 Hz) |
| Detection LS/DLS | Temperature: 30 °C<br>Sampling rate: 5 Hz<br>Correlator run time: 5s<br>Correlator function clip time: 300 µs for LNPs, 10 µs for proteins<br>Laser power: 25% |
| Injection | Injection volume: varied according to sample concentration and size<br>Sample temperature: 4 °C<br>Needle wash: 3 s with 10 % ethanol |

**Note:** Due to their huge particle size, LNPs scatter immensely in LS/DLS and can easily saturate the detector. When analyzing unknown LNP samples, dilute the samples 1:10 or 1:100 and reduce the laser power to 10% to avoid detector saturation. Increase sample amount and laser power step by step.

**Note:** Appropriate correlator function clip time is essential for correct DLS results. For proteins like BSA and antibodies, 10 µs is recommended. For large molecules like LNPs, increase the value to around 300 µs.

## Results and discussion

LNPs usually vary in size from 50 to 200 nm in diameter. To enable separation of potential aggregates and fragments, wide pore sizes of 1,000 to 2,000 nm are used for effective SEC separation. In general, the pore size of the column should be at least three times bigger than the diameter of the molecule of interest. Here, we tested SEC columns with different pore sizes up to 2,000 Å, which equals 200 nm.

For biopharma SEC separations, BSA is the gold standard for column calibration. In addition, BSA is used in static light scattering, as only a single measurement is required for detector calibration procedures as well as for inter-detector delay setup.

The SEC columns were also tested for DLS compatibility, especially with respect to the amount of particle bleeding in the DLS signals observed.

**Note:** If the correlator clip time is increased to 300 µs, the sensitivity for larger particles coming from solvent and columns also increases. For this reason, intensive column purging (directly into waste) is highly recommended for all columns before attaching them to the online DLS flow. Column purging should last a minimum of 12 to 24 hours with a low flow rate of 0.1 or 1.2 mL/min.

Figures 1A–1C show the separation of the BSA monomer, dimer, trimer, tetramer, and higher aggregates on the three different evaluated columns. Excellent resolution between the monomer and the aggregates was found when using the AdvanceBio SEC, 300 Å 7.8 × 300 mm, 2.7 µm column (Figure 1A), in addition to a clean DLS signal. The BSA monomer was further used for calibration and detector setup. Due to the huge size of LNPs, wider pore columns such as the Bio SEC-5, 2,000 Å (Figure 1B) and the PL aquagel-OH MIXED-H (Figure 1C) were tested as well. Both showed less resolution of the BSA sample, as expected. Only one major peak was visible with both columns. In addition, the peak is broader, resulting in lower signal intensity. As DLS is a minor sensitive detector especially suitable for smaller molecules like proteins[6], a much higher sample amount is needed for both wide-pore columns to enable Rh analysis.

The Bio SEC-5, 2,000 Å is the column with the largest pores tested. Here, we see a high number of particles/Rh signals scattering over the complete run time of 20 minutes. This decreases after several more days of washing procedures. The PL aquagel-OH MIXED-H showed a clean signal.

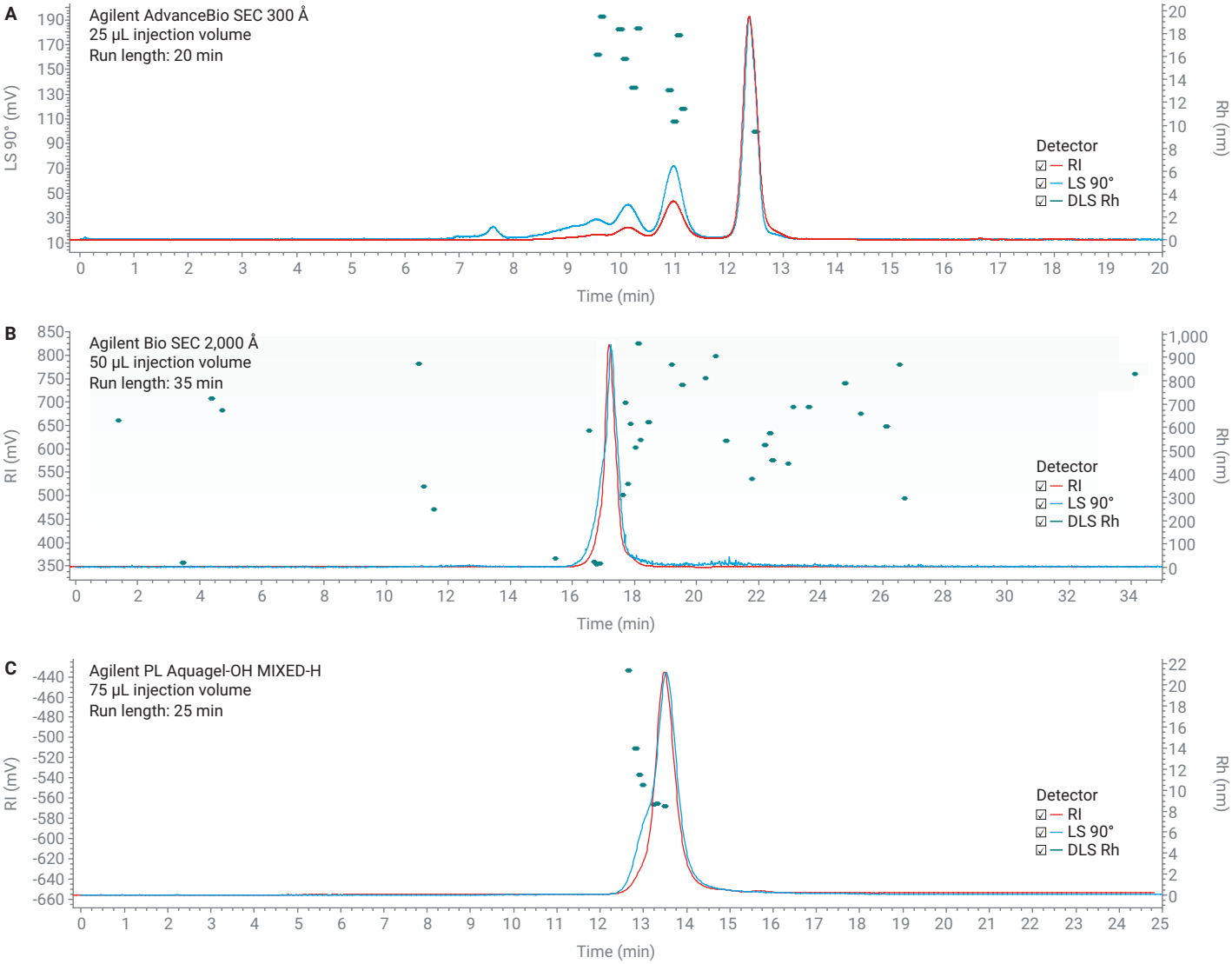


**Figure 1.** BSA (20 mg/mL) separation analysis on three SEC columns A–C, tested for resolution, particle bleed, and sensitivity. The RI signal is in red, the LS 90° signal is in blue, and the DLS Rh signal is represented by green dots.

The same three columns were tested for the analysis of different LNPs. Figure 2 shows the analysis of an empty LNP in the same setup. In contrast to analyzing proteins, the RI signal is very weak for the LNPs compared to the light scattering signals at 90°. Because LNPs are such large molecules, they scatter immensely in light scattering detectors, making it a huge challenge to find a good compromise with respect to dynamic range for the combination of RI and LS/DLS signals.

**Note:** For accurate LS/DLS results, it is very important to work with signals in a reasonable intensity range with good signal-to-noise ratio (at least 50, if possible 200 to 300 mV) for the 90° LS signal. Too weak or too saturated LS signals often result in incorrect MW/Rh results. Therefore, it is critical if the sensitivity of wide-pore columns is not sufficient to gain clear RI signals.

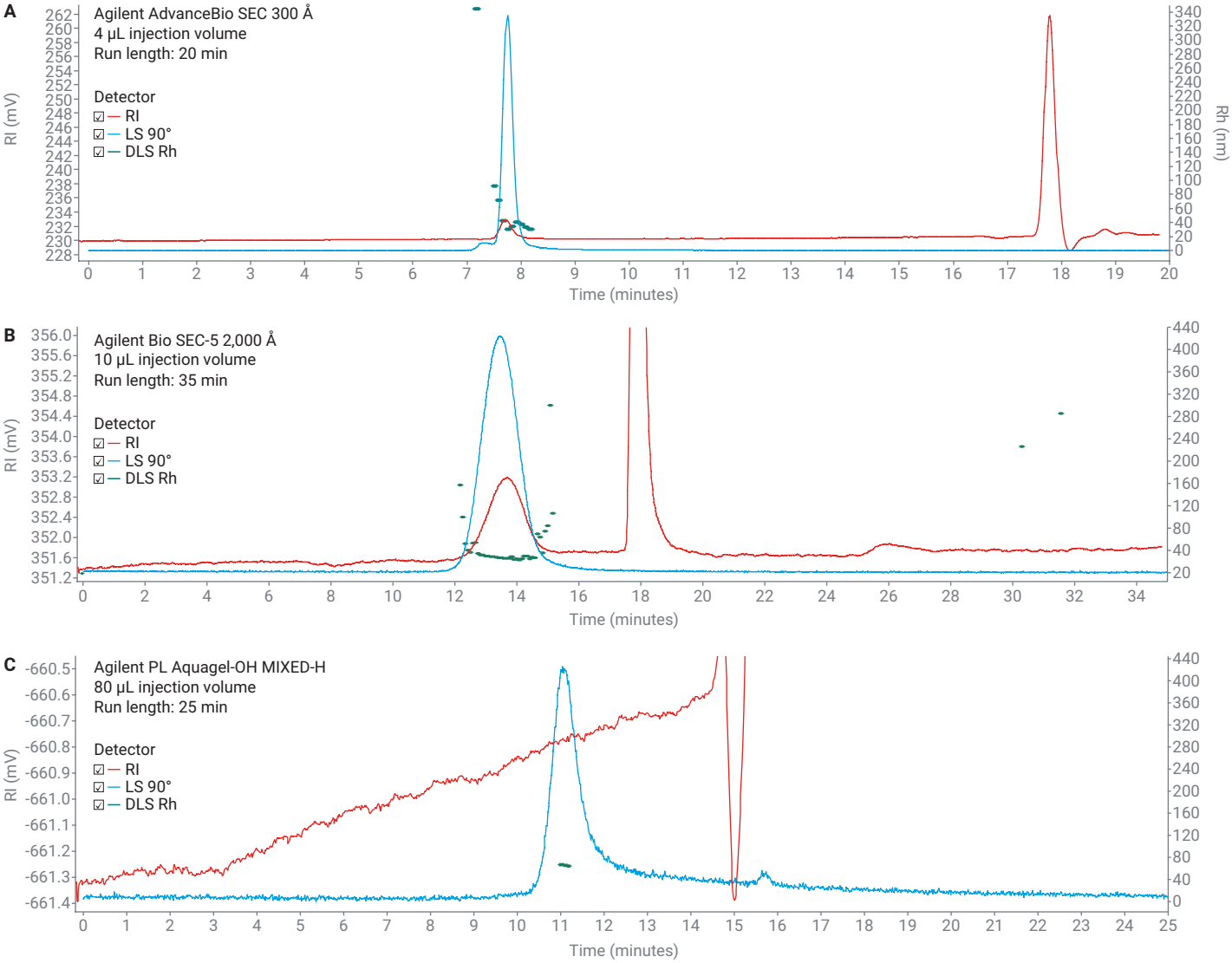


**Figure 2.** Analysis of empty LNP A on three SEC columns A–C, focusing on the different results in resolution, peak shape, and sensitivity. The RI signal is in red, the LS 90° signal is in blue, and the DLS Rh signal is represented by green dots.

Applying the PL Aquagel-OH MIXED-H column did not result in adequate RI signals, even if 20-times higher sample amounts were loaded. Using the Bio SEC-5 column led to better RI results. Some of the tested LNPs showed increased peak tailing on the wide-pore columns, which was not observed on the AdvanceBio SEC, 300 Å column (data not shown).

Interestingly, a separation of a potential aggregate peak was observed for the empty LNP A with the AdvanceBio SEC, 300 Å column (see Figure 2A). Although the pores of the column are too small to enable sufficient SEC separation of these big particles, a separation becomes visible between the main monomer particle and a potential aggregate that was not visible on both wide-pore columns. A possible explanation could be hydrodynamic chromatography (HDC) effects[7] in the tested SEC column. With pores too small for the analyzed LNPs, the stationary phase between the column's pores might act as a non-porous column where different flow speeds lead to separation without using the pores for real SEC separation. This theory needs additional experimental work and evaluation.

The DLS signals as hydrodynamic radius Rh were calculated for all three columns and the results are summarized in Table 2. All LNP sizes were calculated as peak hydrodynamic radius (Rhp). The reference values were the batch DLS values, provided by Merck Life Science KGaA, Darmstadt, Germany. All green values represent deviations from the batch DLS measurement smaller than 15%; deviations over 15% are marked orange. It is clearly visible that the results obtained with the AdvanceBio SEC, 300 Å column are in very close agreement with the batch DLS values, whereas less agreement is found with the two tested wide-pore columns.

**Table 2.** Comparison of Rh values to reference batch DLS measurement. All SEC Rh values below 15% deviation are marked green; deviations above 15% are marked orange.

| Sample Name | Batch DLS Reference Value Rh | Agilent AdvanceBio SEC 300Å Rhp | Agilent Bio-SEC 5 2000Å Rhp | Agilent PL Aquagel-OH MIXED-H Rhp |
|---|---|---|---|---|
| LNP A mRNA | 35 nm | 38 nm | 35 nm | 43 nm |
| LNP B mRNA | 57 nm | 58 nm | 39 nm | 63 nm |
| LNP A (Empty) | 31 nm | 30 nm | 28 nm | 68 nm |
| LNP B (Empty) | 43 nm | 47 nm | 39 nm | 78 nm |

Based on the results shown above, all further experiments were conducted on the AdvanceBio SEC, 300 Å column. In addition to the calculated Rh values, radius of gyration and shape factors were also calculated for the tested LNP samples. The shape factor is defined as Rg/Rh = ρ. For a sphere with a dense core, ρ is expected to be 0.77 or less. All calculated values were evaluated for precision (n = 5) as relative standard deviation (RSD) (see Table 3 and Figure 3).

**Table 3.** Size in Rhp and Rgp and shape factor plus precision values in % RSD for n = 5

| Sample Name | Size Rhp (nm) | RSD (%) | Size Rgp (nm) | RSD (%) | Shape ρ |
|---|---|---|---|---|---|
| LNP A mRNA | 38 | 5.0 | 22.9 | 8.6 | 0.608 |
| LNP B mRNA | 58 | 2.2 | 37.4 | 12.6 | 0.646 |
| LNP A (Empty) | 30 | 2.5 | 25.2 | 15.1 | 0.851 |
| LNP B (Empty) | 47 | 3.2 | 35.1 | 2.1 | 0.752 |

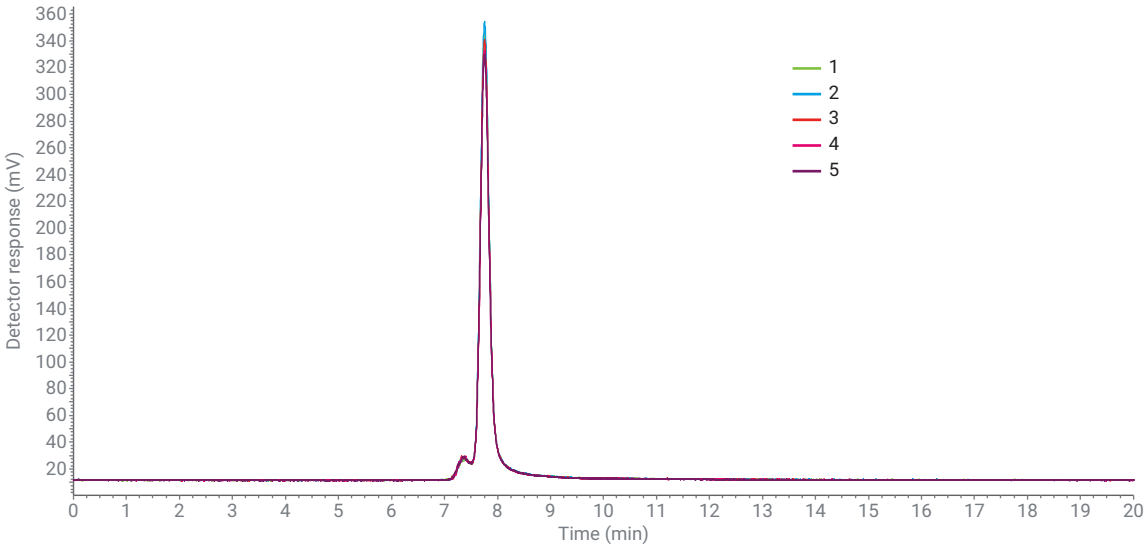


**Figure 3.** Overlay of five consecutive injections of LNP A empty.

Excellent precision was found for the calculated DLS Rhp values. RSD was 5% or less for the tested LNPs, which is extremely precise for this type of measurement. The precision of the measured Rg values was found to be acceptable. The calculated shape factors were also in agreement with the literature values for a dense sphere, except for empty LNP A, which showed a value above 0.77, indicating a change in shape. Looking at empty LNP A, the 90° angle signal already showed a potential aggregation peak (see Figure 2A). To evaluate potential random column interaction or other effects, Figure 3 shows an overlay of five consecutive injections. Here, excellent reproducibility of retention time and area was also observed, leading to the conclusion that the observed aggregation is real and not a column-generated phenomenon.

An important CQA for LNPs is the stability of the particles, which can refer to size changes caused by various conditions like storage time, temperature, light exposure, and other factors. To test the LNPs for stability, the samples were analyzed after three freeze-thaw cycles immediately after thawing with the online SEC-LS/DLS setup. As the samples were sent frozen, two additional freeze-thaw cycles were added in house.

The polydispersity index (PDI) enables the quantification of particle size heterogeneity within a sample. A perfect monodisperse (single size) distribution is indicated by a PDI of 0.0, while a PDI of 1.0 indicates a highly polydisperse (broad size distribution) sample.[8] For LNPs, PDIs below 0.3 are considered acceptable. Table 4 shows the polydispersity index (PDI) values from batch DLS versus Rh values from online SEC-DLS analysis.

For the four different LNP samples tested, only loaded particle B showed consistently perfect monodisperse PDIs over three freeze-thaw cycles. Loaded particle A, as well as both empty LNPs, show increasing PDIs with every freeze-thaw cycle. This is especially prominent in empty particle A, which has indicated potential instability in the other experiments described above.

For the online SEC-DLS analysis, the related RSD values (n = 5) for the Rh measurement were calculated in addition to the corresponding Rh values after three consecutive runs. The empty particles, particularly empty particle A, show less stability, visible in their increasing size but especially in increasing RSD values. This correlates with the batch DLS measured PDI values, which are also visible in Figures 4A and 4B, where the batch DLS PDI values are directly compared with the RSD values from online DLS. Both diagrams look very similar, making Rh RSD values from online SEC-DLS a potential parameter for stability evaluation.

**Table 4.** PDI values from batch DLS versus online SEC-DLS Rh values, plus RSD values obtained from measurement after freeze-thaw cycles.

| | mRNA | | | | Empty | | | |
|---|---|---|---|---|---|---|---|---|
| | LNP A | | LNP B | | LNP A | | LNP B | |
| | Batch DLS | SEC-DLS | Batch DLS | SEC-DLS | Batch DLS | SEC-DLS | Batch DLS | SEC-DLS |
| After Manufacturing | Rh: 35 nm<br>PDI: 0.07 | **N/A** | Rh: 57 nm<br>PDI: 0.04 | **N/A** | Rh: 31 nm<br>PDI: 0.13 | **N/A** | Rh: 43 nm<br>PDI: 0.09 | **N/A** |
| Cycle I | Rh: 36 nm<br>PDI: 0.10 | **Rh: 42 nm<br>RSD 1.5%** | Rh: 57 nm<br>PDI: 0.07 | **Rh: 61 nm<br>RSD 4.6%** | Rh: 32 nm<br>PDI: 0.13 | **Rh: 30 nm<br>RSD 2.5%** | Rh: 44 nm<br>PDI: 0.11 | **Rh: 50 nm<br>RSD 3.2%** |
| Cycle II | Rh: 36 nm<br>PDI: 0.15 | **Rh: 39 nm<br>RSD 3.2%** | Rh: 56 nm<br>PDI: 0.06 | **Rh: 59 nm<br>RSD 4.6%** | Rh: 34 nm<br>PDI: 0.23 | **Rh: 38 nm<br>RSD 17%** | Rh: 44 nm<br>PDI: 0.18 | **Rh: 62 nm<br>RSD 6.5%** |
| Cycle III | Rh: 37 nm<br>PDI: 0.17 | **Rh: 41 nm<br>RSD 6.9%** | Rh: 56 nm<br>PDI: 0.07 | **Rh: 61 nm<br>RSD 7.3%** | Rh: 37 nm<br>PDI: 0.45 | **Rh: 33 nm<br>RSD 14%** | Rh: 45 nm<br>PDI: 0.13 | **Rh: 64 nm<br>RSD 3.8%** |

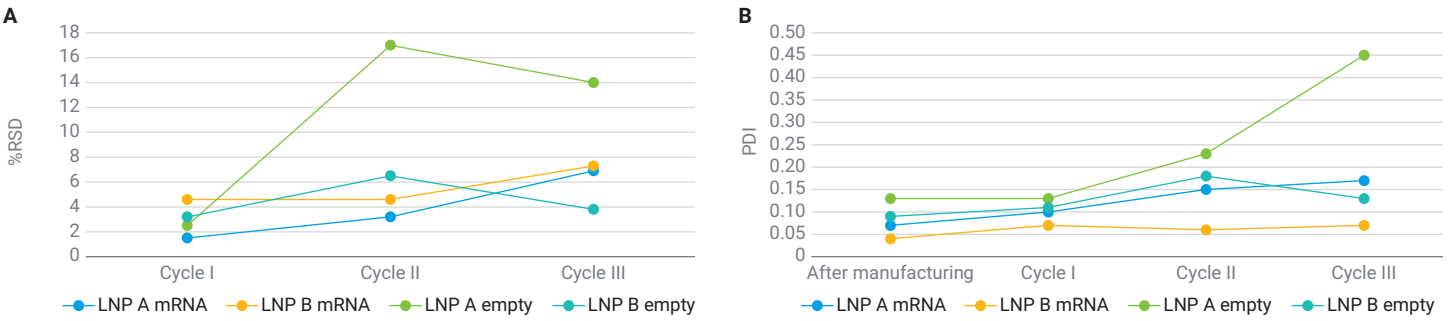


**Figure 4.** PDI values from batch DLS (A) versus RSD values from online SEC-DLS (B) over three freeze-thaw cycles.

### Analysis of targeting moieties of LNPs

The value of having one column to analyze proteins as well as LNPs for size enables the analysis of combined LNP/protein samples. Monoclonal antibodies can be attached to the surface of the LNPs to direct the biopharmaceutical to the right cell target. Figure 5A shows an (RNA-loaded) LNP sample with an additionally bound mAb on the LNP surface. In the purified LNP sample, no free mAb was detected (Figure 5A). Figure 5B shows the analysis of the LNP sample plus spiked mAb solution. The LNP is well separated from the mAb and has been well identified with static light scattering detection, revealing a mass of 166 kDa. Hence, this analysis could be used in quality control to detect free mAb in the LNP formulation.

Figure 5 also clearly shows the difference in signal intensity behavior between protein and LNP samples. The intense scattering of the large LNP samples causes a very high LS signal and very low RI signal, whereas in contrast, the mAb shows a high RI signal intensity and rather low LS signal intensity, underlining the need of a high dynamic range system to enable both DLS and RI analysis.

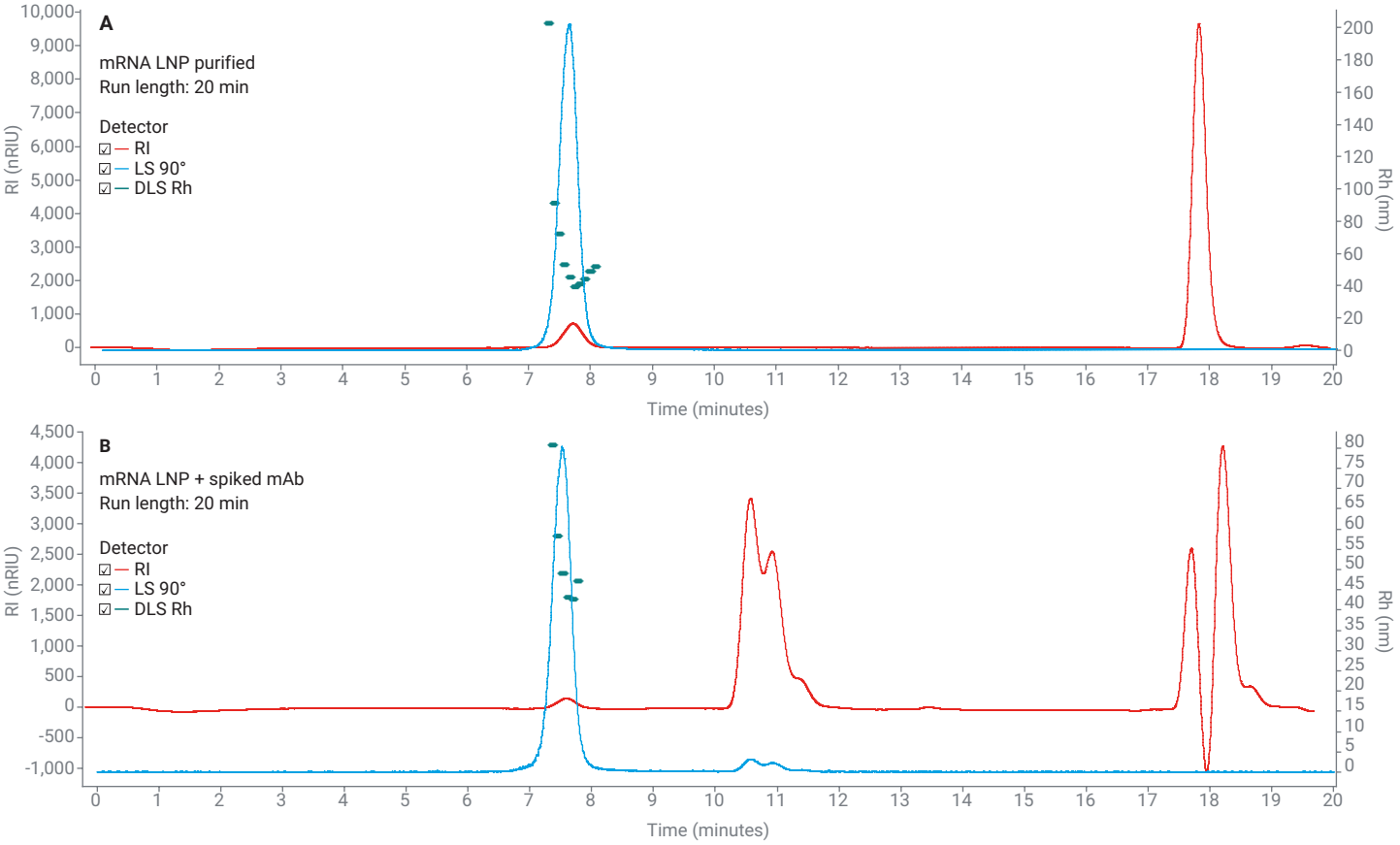


**Figure 5.** (A) purified mRNA LNP sample; (B) spiked mRNA sample with mAb solution.

## Conclusion

The experiments described in this application note revealed several advantages of middle-sized pore columns for the analysis of loaded and empty LNPs in terms of calibration options, peak intensity, and Rh accuracy. Accurate and highly precise Rh values were found in the online SEC-LS/DLS setup for loaded and empty LNPs, providing a reliable method for LNP size determination. High agreement was found in comparison to batch DLS measurements.

Further parameters like aggregation, shape, and stability were successfully evaluated, as well as a special combination of an RNA-loaded LNP plus additional bound mAb. LNP and mAb were baseline separated, and both molecules could be analyzed and identified using online SEC-DLS and static light detection.

The Agilent 1290 Infinity III Bio LC plus Agilent 1260 Infinity II Bio-SEC Multidetector System with advanced light scattering detection, in combination with the Agilent AdvanceBio SEC, 300 Å column, provides a powerful method for the reliable characterization of CQAs of LNPs.

## References


1. Schneider, S. Analysis of Lipid Nanoparticle Composition. *Agilent Technologies application note*, publication number 5994-4709EN, **2022**.
2. Analytical Procedures for Quality of mRNA Vaccines and Therapeutics (Draft Guidelines: 3rd Edition), 2024.
3. Rodriguez-Loya, *et al.* Dynamic Light Scattering and Its Application to Control Nanoparticle Aggregation in Colloidal Systems: A Review. *Micromachines* **2024**, *15*, 24.
4. Mehta, M.; *et al.* Lipid-Based Nanoparticles for Drug/Gene Delivery: An Overview of the Production Techniques and Difficulties Encountered in Their Industrial Development. *ACS Mater. Au* **2023**, *3*, 600–619.
5. Xiujuan, J.; *et al.* Enabling Online Determination of the Size-Dependent RNA Content of Lipid Nanoparticle-Based RNA Formulations. *J. Chrom. B* **2021**, *1186*, 123015.
6. Schneider, S. Determination of Protein Molecular Weight and Size Using the Agilent 1260 Infinity Multi-Detector Bio-SEC Solution with Advanced Light Scattering Detection. *Agilent Technologies application note*, publication number 5991-3955EN, **2014**.
7. Williams, A.; *et al.* Characterisation of nanoparticulate systems by hydrodynamic chromatography. *International Journal of Pharmaceutics*, **2002**, *242*, 295–299.
8. DYNAMIC LIGHT SCATTERING - COMMON TERMS DEFINED. Whitepaper Malvern Panalytical.


**www.agilent.com**


DE-010287



This information is subject to change without notice.

© Agilent Technologies, Inc. 2025



Printed in the USA, October 24, 2025
5994-8735EN


Agilent
Trusted Answers